10156 *Inorg. Chem.* **2010**, *49*, 10156–10165
DOI: 10.1021/ic101435b

Inorganic Chemistry
Article

Antiferromagnetic versus Ferromagnetic Exchange Interactions in Bis(μ-$O_{oximate}$)dinickel(II) Units for a Series of Closely Related Cube Shaped Carboxamideoximate-Bridged Ni_4 Complexes. A Combined Experimental and Theoretical Magneto-Structural Study

M. A. Palacios,[†] Antonio J. Mota,[†] Jesús E. Perea-Buceta,[†] Fraser J. White,[‡] Euan K. Brechin,*[,‡] and Enrique Colacio*[,†]

[†]*Departamento de Química Inorgánica, Facultad de Ciencias, Universidad de Granada, Avenida Fuentenueva S/N, 18071 Granada, Spain, and* [‡]*School of Chemistry, The University of Edinburgh, West Mains Road, Edinburgh EH9 3JJ, United Kingdom*

Received July 19, 2010

The syntheses, crystal structures, and the experimental and theoretical magnetochemical characterization for three tetrametallic Ni(II) clusters, namely, $[Ni_4(L)_4(Cl)_2(MeOH)_2](ClO_4)_2 \cdot 4MeOH$ (**1**), $[Ni_4(L)_4(N_3)_2(MeOH)_2](ClO_4)_2 \cdot 2MeOH$ (**2**), and $[Ni_4(L1)_4(pyz)_2(PhCOO)_2(MeOH)_2](ClO_4)_2 \cdot 7MeOH$ (**3**) (where HL and HL1 represent bipyridine-2-carboxamideoxime and pyrimidine-2-carboxamideoxime, respectively) are reported. Within the Ni_4^{2+} units of these compounds, distorted octahedral Ni(II) ions are bridged by carboxamideoximato ligands to adopt a distorted tetrahedral disposition. The Ni_4^{2+} unit, of C_2 symmetry, can also be viewed as a cube with single [O-atom] and double [NO oxime] bridging groups as atom edges, which define two almost square-planar $Ni(O)_2Ni$ rings and four irregular hexagonal $Ni(NO)_2Ni$ rings. To analyze the magnetic properties of **1**−**3**, we have considered the simplest two-J model, where $J_1 = J_2$ (exchange interactions between the Ni(II) ions belonging to the $Ni(O)_2Ni$ square rings) and $J_a = J_b = J_c = J_d$ (exchange interactions between the Ni(II) ions belonging to the Ni−$(NO)_2$Ni hexagonal rings) with the Hamiltonian $H = -J_1(S_1S_2 + S_3S_4) - J_a(S_1S_3 + S_1S_4 + S_2S_3 + S_2S_4)$. The J_1 and J_a values derived from the fitting of the experimental susceptibility data are $-5.8\ cm^{-1}$ and $-22.1\ cm^{-1}$ for **1**; $-2.4\ cm^{-1}$ and $-22.8\ cm^{-1}$ for **2**, and $+15.6\ cm^{-1}$ and $-10.8\ cm^{-1}$ for **3**. The magneto-structural results and density-functional theory (DFT) calculations demonstrate that the exchange interactions inside the Ni(μ-O)$_2$Ni square rings depend on the Ni−O−Ni bridging angle (θ) and the out-of-plane angle of the NO oximate bridging group with respect to the $Ni(O)_2Ni$ plane (τ), whereas the interactions propagated through the Ni−N−O(Ni)−Ni exchange pathways defining the side of the hexagonal rings depend on the Ni−N−O−Ni torsion angle (α). In both cases, theoretical magneto-structural correlations were obtained, which allow the prediction of the angle for which ferromagnetic interactions are expected. For compound **3**, the existence of the axial magnetic exchange pathway through the *syn-syn* benzoate bridge may also contribute (in addition to the θ and τ angles) to the observed F interaction in this compound through orbital countercomplementarity, which has been supported by DFT calculations. Finally, DFT calculations clearly show that the antiferromagnetic exchange increases when the dihedral angle between the O−Ni−O planes of the Ni(μ-O)$_2$Ni square ring, β, increases.

Introduction

It is well-known that oximate ligands exhibit a great ability to form homo- and heterometallic polynuclear complexes, in which the oximate bridging ligands efficiently transmit magnetic exchange.[1] Among oximate bridging ligands, R-substituted 2-pyridyloximes, (py)C(R)NOH, and salycylaldoximes, R-saoH_2, play an outstanding role as they are able to generate a great variety of polynuclear complexes with aesthetically pleasing structures and interesting magnetic properties, including Single Molecule Magnet (SMM)[1c,2] and Single Chain Magnet (SCM) behavior.[3] In spite of the great potential of pyridine-2-carboxamideoxime, (py)C(NH_2)NOH (see Scheme 1), as a bridging ligand for the formation of cluster complexes, its coordination chemistry remains largely unexplored. With only

*To whom correspondence should be addressed. E-mail: ebrechin@staffmail.ed.ac.uk (E.K.B.), ecolacio@ugr.es (E.C.).

(1) (a) Chaudhuri, P. *Coord. Chem. Rev.* **2003**, *243*, 143. (b) Milios, C. J.; Stamatatos, Th. C.; Perlepes, S. P. *Polyhedron* **2006**, *25*, 134. (c) Milios, C. J.; Piligkos, S.; Brechin, E. K. *Dalton Trans.* **2008**, 1809.

(2) (a) Stamatatos, Th. C.; Foguet-Albiol, D.; Lee, S.-C.; Stoumpos, C. C.; Raptopoulou, C. P.; Terzis, A.; Wernsdorfer, W.; Hill, S. O.; Perlepes, S. P.; Christou, G. *J. Am. Chem. Soc.* **2007**, *129*, 9484. (b) Stamatatos, Th. C.; Foguet-Albiol, D.; Lee, S.-C.; Stoumpos, C. C.; Raptopoulou, C. P.; Terzis, A.; Wernsdorfer, W.; Hill, S. O.; Perlepes, S. P.; Christou, G. *Polyhedron* **2007**, *26*, 2165. (c) Lee, S.-C.; Stamatatos, Th. C.; Hill, S.; Perlepes, S. P.; Christou, G. *Polyhedron* **2007**, *26*, 2225.

(3) Coulon, C.; Miyasaka, H.; Clérac, R. *Struct. Bonding* (*Berlin*) **2006**, *122*, 163. Miyasaka, H.; Julve, M.; Yamashita, M.; Clérac, R. *Inorg. Chem.* **2009**, *48*, 3420.

 Published on Web 10/01/2010

Scheme 1. General Structural Formula for Simple Pyridyl- and Salicyloximes (Top) and for the Carboxamideoxime Ligands Used in This Work (Bottom)

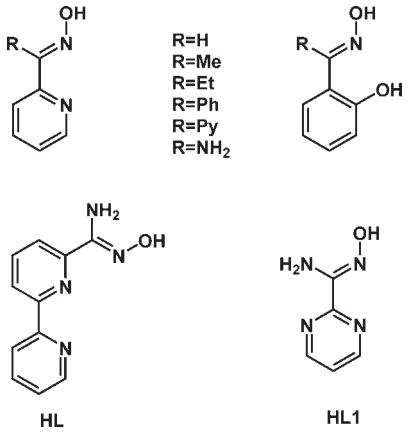

one exception, all the reported complexes of (py)C(NH_2)NOH are mononuclear with the ligand coordinating in a chelating neutral form through the heterocyclic and oxime nitrogen atoms.[1b] Recently, Perlepes and Brechin have succeeded in obtaining the first example of a polynuclear complex where the (py)C(NH_2)NOH ligand adopts four different anionic chelating/bridging coordination modes.[4] Although numerous high nuclearity homometallic complexes bearing R-substituted 2-pyridyloximate ligands have been reported so far, only a few of them contain Ni(II) ions.[5] It should be noted at this point that homometallic polynuclear Ni(II) complexes are the subject of much interest, particularly in the field of molecular magnetism, because they may exhibit SMM behavior,[6] a property which is a result of a large spin ground state that undergoes considerable Ising-type axial magnetic anisotropy (*D*). In spite of the fact that mononuclear Ni(II) complexes can present significant *D* values, only a few examples of nickel(II) SMMs have been reported so far.

Following on from our studies on polynuclear metal complexes with multidentate bridging ligands prepared from 2-cyanopyrimidine and 2-cyanobipyridine synthons,[7] we have used the ligands bipyridine-2-carboxamideoxime (HL) and pyrimidine-2-carboxamideoxime (HL1) (see Scheme 1) for the synthesis of some unusual tetranuclear Ni(II) complexes. The difference in electronic properties and capability to establish hydrogen bonds promoted by the presence of an extra endocyclic nitrogen in the sixth position of the pyrimidine ring in HL1, the existence of exocyclic amine groups in both HL and HL1, as well as the presence of three nitrogen donor atoms in the *mer* disposition in HL, may modify the coordination properties of these ligands with respect to those of the pyridine analogue and, as a consequence, afford polynuclear complexes with new topologies. Herein we report the X-ray structures, magnetic properties, and DFT calculations of three tetrahedral Ni_4 complexes:

$$[Ni_4(L)_4(Cl)_2(MeOH)_2](ClO_4)_2 \cdot 4MeOH \quad (1)$$

$$[Ni_4(L)_4(N_3)_2(MeOH)_2](ClO_4)_2 \cdot 2MeOH \quad (2)$$

$$[Ni_4(L1)_4(pyz)_2(PhCO_2)_2(MeOH)_2](ClO_4)_2 \cdot 7MeOH \quad (3)$$

Experimental Section

General Information. Unless stated otherwise, all reactions were conducted in oven-dried glassware in aerobic conditions, with the reagents purchased commercially and used without further purification. The ligand HL1 was prepared as previously described.[8]

Synthesis of HL. The preparation of 6-carbonitrile-2,2′-bispyridine (**B**) was carried out according to a two-step procedure described previously.[9] Subsequently, conversion of (**B**) into *N*-hydroxy-2,2′-bipyridine-6-carboxamidine (**C**) was achieved as follows:[10] to a solution of (**B**) (2520 mg, 13.9 mmol, 1 equiv) in EtOH (60 mL) at 0 °C were sequentially added hydroxylamine hydrochloride (966 mg, 13.9 mmol, 1.0 equiv) and potassium carbonate (1921 mg, 13.9 mmol, 1 equiv). The resulting reaction mixture was stirred for 5 min under argon, and then heated overnight upon gentle reflux. Concentration in vacuo afforded a white solid residue which was throughoughly extracted with a mixture of CH_2Cl_2/MeOH (4:1). The combined extracts were evaporated giving a yellow solid which was further purified by recrystallization from Et_2O/hexane (1:1) to provide a pure white-yellow powder (**C**) (1173 mg, 72% yield). (**C**) **IR** (KBr) υmax (cm^{-1}), 3464, 3359, 3093, 2822, 1655, 1581, 1568, 1547, 1470, 1381, 1262. 1169, 1141, 1082; **^{1}H NMR** (400 MHz, $(CD_3)_2SO$) δ 5.94−6.18 (2H, m, N***H***-O***H***), 7.47 (1H, dd, J = 15.1, 21.1 Hz, C-5′ (*H*)), 7.81−8.03 (3H, m, C-4(*H*), C-4′(*H*), C-5(*H*)), 8.39 (1H, d, J = 7.4 Hz, C-6′(*H*)), 8.61−8.74 (2H, m,C-3′(*H*), C-3(*H*)), 9.97 (1H, s, -C=N***H***); **^{13}C NMR** (101 MHz, $(CD_3)_2SO$ δ 119.7 (**C**H-3′), 120.4 (**C**H-5′), 121.1 (**C**H-5), 124.4 (**C**H-3), 137.7 (**C**H-4′), 137.7 (**C**H-4), 149.2 (**C**H-6′), 149.5 (**C**(NHOH)=NH), 149.7 (**C**-6), 153.4 (**C**-2), 154.8 (**C**-2′); Anal. Calcd. (Found) for $C_{11}H_{10}N_4O$ (**C**): C, 61.67 (61.30); H, 4.71 (4.98); N, 26.15 (25.82).

The ligand HL can exhibit two tautomeric forms. One is that given in Scheme 1, and the other one is that shown in Scheme 2C. The NMR data point out that the latter is the major tautomeric form in $(CD_3)_2SO$ solution.

(4) Papatriantafyllopoulou, C.; Jones, L. F.; Nguyen, T. D.; Matamoros-Salvador, N.; Cunha-Silva, L.; Almeida Paz, F. A.; Rocha, J.; Evangelisti, M.; Brechin, E. K.; Perlepes, S. *Dalton Trans.* **2008**, 3153.

(5) (a) Stamatatos, Th. C.; Escuer, A.; Abboud, K. A.; Raptopoulou, C. P.; Perlepes, S. P.; Christou, G. *Inorg. Chem.* **2008**, *47*, 11825. (b) Chaudhuri, P.; Weyhermüller, T.; Wagner, R.; Khanra, S.; Biswas, B.; Bothe, E.; Bill, E. *Inorg. Chem.* **2007**, *46*, 9003. (c) Stamatatos, Th. C.; Papatriantafyllopoulou, C.; Katsoulakou, E.; Raptopoulou, C. P.; Perlepes, S. P. *Polyhedron* **2007**, *26*, 1830. (d) Stamatatos, Th. C.; Diamantopoulou, E.; Tasiopoulos, A. J.; Psycharis, V.; Vicente, R.; Raptopoulou, C. P.; Nastopoulos, V.; Escuer, A.; Perlepes, S. P. *Inorg. Chim. Acta* **2006**, *359*, 4149. (e) Stamatatos, Th. C.; Diamantopoulou, E.; Raptopoulou, C. P.; Psycharis, V.; Vicente, R.; Escuer, A.; Perlepes, S. P. *Inorg. Chem.* **2007**, *46*, 2350. (f) Weyhermüller, T.; Wagner, R.; Khanra, Chaudhuri, P. *Dalton Trans.* **2005**, 2539. (g) Khanra, S.; Weyhermüller, T.; Rentschler, E.; Chaudhuri, P. *Inorg. Chem.* **2005**, *44*, 8176. (h) Biswas, B.; Pieper, U.; Weyhermüller, T.; Chaudhuri, P. *Inorg. Chem.* **2009**, *48*, 6781. (i) Stamatatos, Th. C.; Abboud, K. A.; Perlepes, S. P.; Christou, G. *Dalton Trans.* **2007**, 3861. (j) Zhang, S.; Zhen, L.; Xu, B.; Inglis, R.; Li, K.; Chen, W.; Zhang, Y.; Konidaris, K. F.; Perlepes, S. P.; Brechin, E. K.; Li, Y. *Dalton Trans.* **2010**, *39*, 3563.

(6) Scott, R. T. W.; Jones, L. F.; Tidmarsh, I. S.; Breeze, B.; Laye, R. H.; Wolowska, J.; Stone, D. J.; Collins, A.; Parsons, S.; Wernsdorfer, W.; Aromí, G.; McInnes, E. J. L.; Brechin, E. K. *Chem.—Eur. J.* **2009**, *15*, 12389.

(7) (a) Rodríguez, A.; Kivekäs, R.; Colacio, E. *Chem. Commun.* **2005**, 5228. (b) Rodríguez, A.; Palacios, M. A.; Sironi, A.; Colacio, E. *Dalton Trans.* **2008**, 2887. (c) Rodríguez-Diéguez, A.; Salinas-Castillo, A.; Galli, S.; N. Masciocchi, N.; Gutiérrez-Zorrilla, J. M.; Vitoria, P.; Colacio, E. *Dalton Trans.* **2007**, 1821. (d) Rodríguez-Diéguez, A.; Cano, J.; Kivekäs, R.; Debdoubi, A.; Colacio, E. *Inorg. Chem.* **2007**, *46*, 2503.

(8) Rodríguez-Diéguez, A.; Kivekäs, R.; Sakiyama, H.; Debdoubi, A.; Colacio, E. *Dalton Trans.* **2007**, *46*, 2503.

(9) Norrby, T.; Börje, A.; Zhang, L.; Åkermark, B. *Acta Chem. Scand.* **1998**, *52*, 77–85.

(10) Bentiss, F.; Lagrenée, M.; Traisnel, M.; Mernari, B.; Elattari, H. *J. Heterocyclic. Chem.* **1999**, *36*, 149–152.

Scheme 2. Synthesis of the Ligand HL

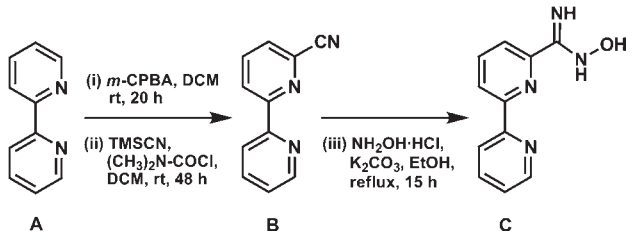

Preparation of Complexes (1)−(3). **$[Ni_4(L)_4(Cl)_2(MeOH)_2](ClO_4)_2\cdot 4MeOH$ (1).** HL (0.100 g, 0.467 mmol), NH_4ClO_4 (0.055 g, 0.467 mmol), and $NiCl_2$ (0.061 g, 0.467 mmol) were added to 30 mL of methanol with continuous stirring. After a few minutes, Et_4NOH (0.147 g, 1 mmol) was added, and the mixture stirred for 2 h. The resulting orange solid was filtered off, and the filtrate kept at room temperature for a week to afford brown crystals suitable for X-ray diffraction. Crystals were filtered, washed with methanol, and air-dried. Anal. Calcd. for $C_{50}H_{58}Cl_4N_{16}Ni_4O_{18}$: C, 38.76; H, 3.74; N, 14.48. Found: C, 38.94; H, 3.68; N, 14.87; IR (KBr, cm^{-1}): 3443, 3360 ν(NH); 1604, ν(C=C); 1091 $\nu(ClO_4)$.

$[Ni_4(L)_4(N_3)_2(MeOH)_2](ClO_4)_2\cdot 2MeOH$ (2). HL (0.100 g, 0.467 mmol), NH_4ClO_4 (0.055 g, 0.467 mmol), $NiCl_2$ (0.061 g, 0.467 mmol) and NaN_3 (0.061 g, 1 mmol) were added to 30 mL of methanol with continuous stirring. After a few minutes, Et_4NOH (0.147 g, 1 mmol) was added, and the mixture stirred for 2 h. The solution was filtered to eliminate any insoluble material, and the filtrate allowed to stand at room temperature. X-ray quality brown crystals of **2** were obtained by slow evaporation of the solution after several days. Crystals were filtered, washed with methanol, and air-dried. Anal. Calcd. for $C_{48}H_{52}Cl_2N_{22}Ni_4O_{16}$: C, 38.42; H, 3.46; N, 20.54. Found: C, 38.16; H, 3.07; N, 20.41; IR (KBr, cm^{-1}): 3456, 3360 ν(NH); 2038 ν(N3); 1604, ν(C=C); 1078 $\nu(ClO_4)$.

$[Ni_4(L1)_4(pyz)_2(PhCOO)_2(MeOH)_2](ClO_4)_2\cdot 7MeOH$ (3). HL1 (0.138 g, 1 mmol), NH_4ClO_4 (0.130 g, 1 mmol), $NiCl_2$ (0.117 g, 1 mmol), pyrazine (0.08 g, 1 mmol), and sodium benzoate (0.144 g, 1 mmol) were added to 30 mL of methanol with continuous stirring. After a few minutes, Et_4NOH (0.294 g, 2 mmol) was added, and the mixture stirred for 2 h. The resulting red solid was filtered off, and the filtrate was allowed to stand at room temperature for several days, whereupon brown crystals of **3** were obtained. Crystals were filtered, washed with methanol and air-dried. Anal. Calcd. for $C_{51}H_{74}Cl_2N_{20}Ni_4O_{25}$: C, 37.14; H, 4.49; N, 16.99. Found: C, 37.24; H, 4.68; N, 16.87; IR (KBr, cm^{-1}): 3472, 3342 ν (NH); 1600, ν(C=C); 1095 $\nu(ClO_4)$.

Computational Details. All theoretical calculations were carried out at the DFT level of theory using the hybrid B3LYP exchange-correlation functional,[11] as implemented in the Gaussian 03 program.[12] A quadratic convergence method was employed in the self-consistent field (SCF) process.[13] The triple ζ quality basis set proposed by Ahlrichs and co-workers has been used for all atoms.[14] Calculations were performed on the complexes built from the experimental geometries as well as on model complexes. The electronic configurations used as starting points were created using the Jaguar 7.6 software.[15] The approach used to determine the exchange coupling constants for polynuclear complexes has been described in detail elsewhere.[16]

Physical Measurements. Elemental analyses were carried out at the "Centro de Instrumentación Científica" (University of Granada) on a Fisons-Carlo Erba analyzer model EA 1108. The IR spectra on powdered samples were recorded with a Thermo-Nicolet IR200FTIR by using KBr pellets. Magnetization and variable temperature (2−300 K) magnetic susceptibility measurements on polycrystalline samples were carried out with a Quantum Design SQUID MPMS XL-5 device operating at different magnetic fields. The experimental susceptibilities were corrected for the diamagnetism of the constituent atoms by using Pascal's tables.

Single-Crystal Structure Determination. Suitable crystals of **1**−**3** were mounted on glass fiber and used for data collection. Data were collected with a dual source Oxford Diffraction SuperNova diffractometer equipped with an Atlas CCD detector and an Oxford Cryosystems low temperature device operating at 100 K. Mo K_α radiation (λ = 0.71073 Å) was used to collect data for **1** and **2** and Cu K_α (λ = 1.5418 Å) was used for **3**. Semiempirical (multiscan) absorption corrections were applied for **1** and **2**, and a face-indexed absorption correction was applied for **3** in both cases using Crysalis Pro.[17] The structures were solved by direct methods[18] and refined with full-matrix least-squares calculations on F^2.[19] The Ni_4^{2+}-cations were well resolved in the structure of **3** but the counteranions and solvent molecules were not. Instead, a new set of F^2 (hkl) values with the contribution from solvent molecules and perchlorate anions withdrawn were obtained by the SQUEEZE procedure implemented in PLATON_94.[20] Anisotropic temperature factors were assigned to all atoms but the hydrogens, which are riding their parent atoms with an isotropic temperature factor arbitrarily chosen as 1.2 times that of the respective parent. Final $R(F)$, $wR(F^2)$ and goodness of fit agreement factors, details on the data collection, and analysis can be found in Table 1.

Results and Discussion

The reaction between the ligand HL and $NiCl_2$ in a 1:1 molar ratio and in the presence of an excess of base (Et_4NOH) affords the tetranuclear complex **1**, in which the ligand, as expected, is deprotonated and acts as a bridge between the Ni(II) ions. In an attempt to introduce end-on azide-bridging groups in the

(11) (a) Becke, A. D. *Phys. Rev. A* **1988**, *38*, 3098. (b) Lee, C. T.; Yang, W. T.; Parr, R. G. *Phys. Rev. B* **1988**, *37*, 785. (c) Becke, A. D. *J. Chem. Phys.* **1993**, *98*, 5648.

(12) Frisch, M. J.; Trucks, G. W.; Schlegel, H. B.; Scuseria, G. E.; Robb, M. A.; Cheeseman, J. R.; Montgomery, Jr., J. A.; Vreven, T. ; Kudin, K. N.; Burant, J. C.; Millam, J. M.; Iyengar, S. S.; Tomasi, J.; Barone, V.; Mennucci, B.; Cossi, M.; Scalmani, G.; Rega, N.; Petersson, G. A.; Nakatsuji, H.; Hada, M.; Ehara, M.; Toyota, K.; Fukuda, R.; Hasegawa, J.; Ishida, M.; Nakajima, T.; Honda, Y.; Kitao, O.; Nakai, H.; Klene, M.; Li, X.; Knox, J. E.; Hratchian, H. P.; Cross, J. B.; Adamo, C.; Jaramillo, J.; Gomperts, R.; Stratmann, R. E.; Yazyev, O.; Austin, A. J.; Cammi, R.; Pomelli, C.; Ochterski, J. W.; Ayala, P. Y.; Morokuma, K.; Voth, G. A.; Salvador, P.; Dannenberg, J. J.; Zakrzewski, V. G.; Dapprich, S.; Daniels, A. D.; Strain, M. C.; Farkas, O.; Malick, D. K.; Rabuck, A. D.; Raghavachari, R.; Foresman, J. B.; Ortiz, J. V.; Cui, Q.; Baboul, A. G.; Clifford, S.; Cioslowski, J.; Stefanov, B. B.; Liu, G.; Liashenko, A.; Piskorz, P.; Komaromi, I.; Martin, R. L.; Fox, D. J.; Keith, T.; Al-Laham, M. A.; Peng, C. Y.; Nanayakkara, A.; Challacombe, M.; Gill, P. M. W.; Johnson, B.; Chen, W.; Wong, M. W.; Gonzalez, C.; Pople, J. A. *Gaussian 03*, Revision C.02; Gaussian, Inc.: Wallingford, CT, 2004.

(13) Bacskay, G. B. *Chem. Phys.* **1981**, *61*, 385.

(14) Schäfer, A.; Huber, C.; Ahlrichs, R. *J. Chem. Phys.* **1994**, *100*, 5829.

(15) *Jaguar*, 7.6; Schrödinger, Inc.: Portland, OR, 2009.

(16) (a) Ruiz, E.; Cano, J.; Alvarez, S.; Alemany, P. *J. Comput. Chem.* **1999**, *20*, 1391. (b) Ruiz, E.; Alvarez, S.; Rodríguez-Fortea, A.; Alemany, P.; Puoillon, Y.; Massobrio, C. In *Magnetism: Molecules to Materials*; Miller, J. S., Drillon, M., Eds.; Wiley-VCH: Weinheim, 2001; Vol. *II*, p 5572. (c) Ruiz, E.; Rodríguez-Fortea, A.; Cano, J.; Alvarez, S.; Alemany, P. *J. Comput. Chem.* **2003**, *24*, 982. (d) Ruiz, E.; Alvarez, S.; Cano, J.; Polo, V. *J. Chem. Phys.* **2005**, *123*, 164110.

(17) *CrysAlis Pro Software system*, Version 1.171.33.55; Oxford Diffraction Ltd.: Abingdon, U.K., 2007; Supernova CCD system.

(18) Altomare, A.; Cascarano, G.; Giacovazzo, C.; Guagliardi, A.; Moliterni, A. G. G.; Burla, M. C.; Polidori, G.; Cavalli, M.; Spagna, R. *SIR97: package for structure solution by direct methods*; University of Bari: Bari, Italy, 1997.

(19) Sheldrick, G. M. *SHELX97: program for crystal structure refinement*; University of Göttingen: Göttingen, Germany, 1997.

(20) Spek, A. L. *PLATON-94, A Multipurpose Crystallographic Tool*, V-101094; University of Utrecht: Utrecht, The Netherlands, 1994.

Table 1. Crystallographic Data for Complexes **1**−**3**

	1	**2**	**3**
chemical formula	$C_{50}H_{58}Cl_4N_{16}Ni_4O_{18}$	$C_{48}H_{52}Cl_2N_{22}Ni_4O_{16}$	$C_{51}H_{74}Cl_2N_{20}Ni_4O_{25}$
M/gmol^{-1}	1547.76	1498.86	1545.04
T(K)	100 (2)	100 (2)	100 (2)
λ/Å	0.71073	0.7107	1.5418
cryst syst	monoclinic	orthorhombic	orthorhombic
space group	*C*2/*c*	*Pbca*	*Pnca*
a/Å	17.9186(6)	13.9395(2)	18.1300(4)
b/Å	23.8467(10)	24.2919(3)	25.3252(5)
c/Å	14.5107(6)	33.8474(4)	14.4407(5)
α/deg	90	90	90
β/deg	93.254(3)	90	90
γ/deg	90	90	90
V/Å^3	6190.4(4)	11461.3(3)	6630.4(3)
Z	4	8	4
ρ(g cm^{-3})	1.661	1.737	1.548
μ(mm^{-4})	1.454	1.478	2.702
unique reflections	17843	108383	25745
R (int)	0	0.0374	0.0335
GOF on F^2	1.028	1.080	1.093
R1[a][$I > 4\sigma(I)$]	0.0657	0.0291	0.0386
wR2[a] [$I > 4\sigma(I)$]	0.1823	0.0796	0.1106

[a] $R(F) = \sum||F_o| - |F_c||/\sum|F_o|$, $wR(F^2) = [\sum w(F_o^2 - F_c^2)^2/\sum wF_o^4]^{1/2}$.

structure that could potentially propagate ferromagnetic interactions, we then carried out the same reaction as for the synthesis of **1** but in the presence of an equimolecular amount of sodium azide. However, the reaction did not lead to the expected product but to **2**, which was formed by the simple substitution of the terminal chloride ligands in **1** by monodentate azide ligands. The ligand HL can coordinate a metal ion in a tridentate form through the endocyclic nitrogen atoms of the bipyridine moiety and the oxime nitrogen atom. The ligand HL1, however, can only be coordinated to a metal ion in a bidentate manner through one of the endocyclic nitrogen atoms of the pyrimidine ring and the oximate nitrogen atom. Owing to this coordination mode of HL1, additional peripheral ligands are needed to saturate the octahedral coordination sphere of the Ni(II) ions. Bearing this in mind, we performed the reaction between HL and $NiCl_2$ in a 1:1 molar ratio and in the same conditions as for **1** and **2** but adding equimolecular amounts of pyrazine and sodium benzoate, which can act as both monodentate and bridging ligands. From the reaction, the tetranuclear complex **3** was obtained, which contains deprotonated HL1 ($L1^-$) and benzoate bridging ligands as well as monodentate pyrazine ligands. We suppose that there might be a number of other HL and HL1-containing high-nuclearity Ni(II) complexes available with subtle differences in their core, as has been shown to occur for R-substituted 2-pyridyloximes in Ni(II) chemistry.[5] The formation of these species depend, among other factors, on the solvent (a change in the solvent polarity could decrease/increase the nuclearity of the Ni(II) complexes because of their different solubility), the ancillary ligands (X), the HL(HL1)/Ni/X ratio, and the method of preparation (hydrothermal or room pressure methods). Our belief is that we are only at the beginning of a long journey in HL(HL1)/Ni/X chemistry.

All of the spectroscopic and analytical data are consistent with the formulation of complexes **1**−**3**.

Crystal Structures. The structure of **1** consists of a $[Ni_4(L)_4(Cl)_2(MeOH)_2]^{2+}$ tetranuclear cationic unit (hereafter Ni_4^{2+}), two perchlorate anions, and four methanol molecules (Figure 1). The counteranions and solvent molecules will not be further discussed.

Within the Ni_4^{2+} units, the distorted octahedral Ni(II) ions are bridged by bipyridine-2-carboxamideoximato ligands (L^-) to adopt a distorted tetrahedral disposition. The Ni_4^{2+} moiety can also be viewed as a cube with single [O-atom] and double [NO oxime] bridging groups as atom edges (Figure 1, right). The L^- ligand is coordinated to a Ni(II) ion through the two bipyridine and the oxime nitrogen atoms in a *mer* disposition, whereas the oximato oxygen atom bridges two different neighboring Ni(II) ions. Therefore, L^- acts in a κ^3-N1,N8,N15:κ^1-O16:κ^1-O16 coordination mode (see Scheme 3, left).

This coordination mode affords two almost square-planar $Ni(O)_2Ni$ rings and four irregular hexagonal $Ni(NO)_2N$ rings inside the Ni_4^{2+} unit of C_2 symmetry, the C_2 axis passing through the center of the two parallel square-planar $Ni(O)_2Ni$ rings (Figure 1, right).

These parallel rings are twisted by approximately 90° with respect to each other such that the bridging oxygen atoms of one ring are located on the Ni(II) ions of the other. The remaining positions on the octahedral Ni(II) ions are occupied by two single oximato oxygen bridging atoms belonging to the same $Ni(O)_2Ni$ ring in *cis* positions and either a chloride or a MeOH molecule. It should be noted that the Ni(II) ions of the same $Ni(O)_2Ni$ ring display the same monocoordinated ligand (either chloride or MeOH). Therefore, in one of the $Ni(O)_2Ni$ rings, the Ni(II) ions exhibit a NiN_3O_2Cl coordination environment, while in the other the coordination sphere is of the NiN_3O_3 type. The Ni···Ni distances and Ni−O−Ni angles inside the $Ni(O)_2Ni$ rings are 3.179 Å and 100.7° for the ring bearing chloride anions and 3.138 Å and 99.6° for the ring bearing methanol molecules. The nitrogen atoms of the NO oximate bridging groups are displaced from each of the planar $Ni(O)_2Ni$ rings (calculated as the Ni−Ni−O−N torsion angle, τ) by 64.1° and 62.9° and by 63.5° and 62.7°, respectively. The Ni···Ni distances for Ni(II) ions across the hexagonal rings are 3.609 Å (for the less distorted hexagonal rings) and 4.039 Å (for the more distorted hexagonal rings). Finally, the Ni−O−N−Ni torsion angles for the hexagonal rings are 38.2° and 39.7° (for the less distorted) and 70.9° and 71.2° (for the more distorted), respectively.

The structure of **2** is very similar to that of **1**, but bearing monocoordinated azide anions instead of chloride anions (Figure 2). Besides this, the most evident differences between structures are as follows: (i) compound **2** has a pseudo C_2 axis passing through the center of the more distorted hexagonal rings; (ii) the Ni(II) ions of the same $Ni(O)_2Ni$ square planar ring have a different monocoordinated ligand (azide and MeOH) and therefore, there are two different coordination environments (NiN_4O_2 and *mer*-NiN_3O_3) for the same $Ni(O)_2Ni$ square planar ring (Figure 2).

The Ni−O−Ni angles in the two $Ni(O)_2Ni$ square planar rings are 99.3° and 100.2°, and 99.1° and 100.6°, with Ni···Ni distances of 3.168 Å and 3.165 Å and τ angles in the ranges 62.8°−67.5° and 63.2°−66.7°, respectively. On the other hand, the Ni−O−N−Ni torsion angles in the hexagonal rings are in the ranges 34.1°−41.6° and 68.3°−73.0°. The Ni···Ni distances for Ni(II) ions across the hexagonal rings are 3.591 Å and 3.602 Å (for the less distorted ring) and 4.037 Å and 4.014 Å (for the more distorted ring).

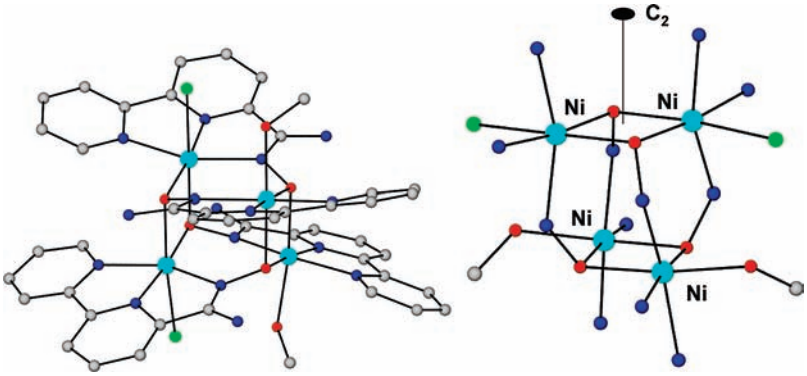

Figure 1. Perspective view of the molecular structure of the cation **1** (left) and Ni_4^{2+} core (right). Nickel, oxygen, nitrogen, chloride, and carbon atoms are in light blue, red, dark blue, green and gray, respectively. Perchlorate and methanol molecules have been omitted for the sake of clarity.

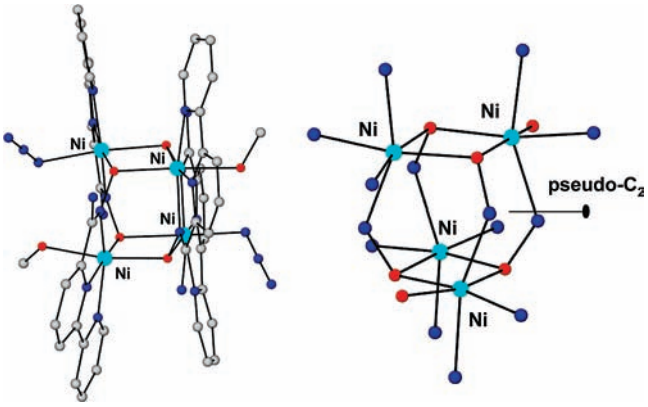

Figure 2. Perspective view of the molecular structure of **2** (left) and its Ni_4^{2+} core (right). Nickel, oxygen, nitrogen, and carbon atoms are in light blue, red, dark blue, and gray, respectively. Perchlorate and solvent molecules are omitted for the sake of clarity.

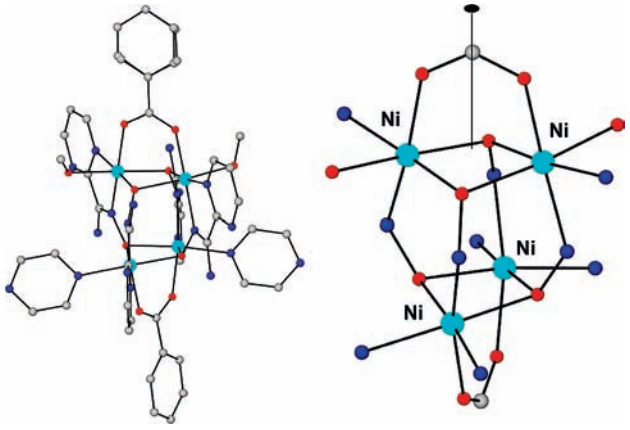

Figure 3. Perspective view of the molecular structure of **3** (left) and its Ni_4^{2+} core (right). Color code as per Figure 1.

Scheme 3. Coordination Modes of the Ligands HL (Left) and HL1 (Right)

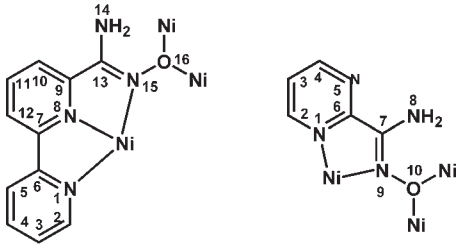

The structure of **3** (Figure 3) is made of a $[Ni_4(L1)_4(pyz)_2(PhCOO)_2(MeOH)_2]^{2+}$ tetranuclear unit, two perchlorate anions, and seven methanol molecules. The oximate-bridged Ni_4^{2+} core of **3** is similar to that of **1** and **2**, exhibiting a "cube" like shape and a tetrahedral distorted arrangement of Ni(II) ions. Within the Ni_4^{2+} unit, the $L1^-$ ligand exhibits a κ^2-N1,N9:k-O10:k-O10 chelating/bridging mode (see Scheme 3, right). Because the $L1^-$ ligand only has two nitrogen donor atoms (pyrimidine and oxime nitrogen atoms) instead of the three of the L^- ligand, additional peripheral ligands are required (*syn-syn* benzoate bridges and monodentate pyrazine) to saturate the coordination sites on the octahedral Ni(II) ions. The Ni_4^{2+} moiety has C_2 symmetry, the 2-fold axis passing through the carbon atom of the *syn-syn* carboxylate group and the center of each square-planar $Ni(O)_2Ni$ ring. Therefore, in one of the $Ni(O)_2Ni$ rings, the Ni(II) ions exhibit a NiO_4N_2 coordination environment, while in the other the coordination sphere is of the NiN_3O_3 type, with a *fac* disposition of the donor atoms (Figure 3). It is interesting to note that the *syn-syn* bridging coordination of the benzoate ligand to the Ni(II) ions of the same $Ni(O)_2Ni$ square planar ring provokes some significant changes in the structural parameters of the $Ni(O)_2Ni$ ring with respect to those observed for compounds **1** and **2**: (i) a considerable shortening of the Ni···Ni distances (3.043 Å and 3.015 Å), (ii) a decrease in the Ni−O−Ni angles (94.2° and 95.1°), and (iii) a significant hinge distortion of the $Ni(O)_2Ni$ square planar ring (with a dihedral angle of 15.9°). The Ni···Ni distances for the Ni(II) ions across the hexagonal rings are also longer than those observed for **1** and **2**, with values of 3.813 Å and 4.064 Å. The out-of-plane displacements of the N atoms of the NO oximate bridging groups from the $Ni(O)_2Ni$ plane (τ angle) are 56.1° and 59.0° for one $Ni(O)_2Ni$ unit and 58.7° and 55.7° for the other. Finally, the Ni−O−N−Ni torsion angles in the hexagonal rings are 41.5° and 41.7°, and 68.3° and 69.2°.

It should be noted at this point that only two oximate-bridged cube-like Ni_4 complexes analogous to **1**−**3** have been reported previously, namely, $[Ni_4(O_2CMe)_2\{(py)_2CNO\}_4](SCN)(OH)\cdot 2.2MeOH\cdot 1.7H_2O$[5e] and $[Ni_4(O_2CMe)_4\{(py)C(Ph)NO\}_4(MeOH)_2]$.[5c] The structure of these compounds, bearing two *syn-syn* acetate bridging groups connecting the Ni(II) ions of the same $Ni(O)_2Ni$ square ring, are somewhat similar to that of **3**.

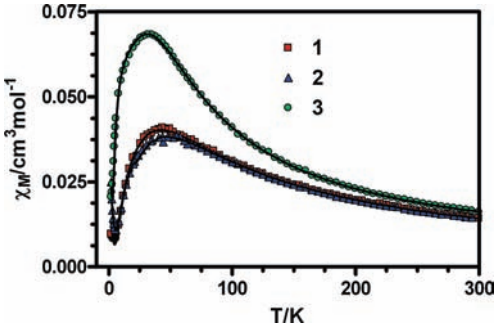

Figure 4. Temperature dependence of χ_M for complexes **1**−**3**.

Scheme 4. Six-*J* and Two-*J* Models for Compounds **1**−**3**

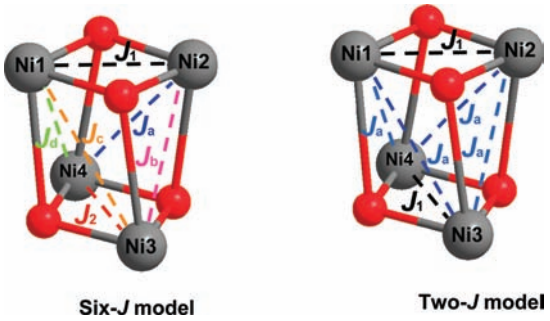

Magnetic Properties

The temperature dependence of χ_M (the molar magnetic susceptibility per Ni_4 unit) for dried microcrystalline samples of compounds **1**−**3** in the range 300−2 K under an applied field of 0.5 T is shown in Figure 4.

The χ_M versus T plots for **1**−**3** show a maximum at 43, 44, and 32 K, respectively, indicating the existence of dominant antiferromagnetic (hereafter AF) interactions between the nickel(II) ions through the oximate bridges. Below the temperature of the maximum, χ_M decreases with decreasing the temperature. At very low temperature, however, χ_M slightly increases, which indicates the presence of a small amount of paramagnetic impurity. As expected, the $\chi_M T$ product for compounds **1**−**3** decreases monotonically from 4.24, 4.30, and 4.82 cm^3 K mol^{-1} at room temperature, respectively, upon cooling down to a value approaching 0 cm^3 K mol^{-1} at 2 K. The lowest temperature values strongly support an $S = 0$ spin ground state for all three complexes. In principle, a maximum of six different J values could be considered for compounds **1**−**3** (see Scheme 4): (i) J_1 and J_2, that correspond to the exchange interactions between Ni1/Ni2 and Ni3/Ni4 metal ions inside the square $Ni(O)_2Ni$ rings propagated by two monatomic oximate bridges, and (ii) J_a, J_b, J_c, and J_d that represent the exchange interactions involving the Ni2/Ni4, Ni2/Ni3, Ni1/Ni3, and Ni1/Ni4 couples of metal ions mediated by two Ni−N−O−Ni oximate bridges, respectively, which are sides of each (Ni−N−O−Ni−O−N) hexagonal ring (see Figures 1, 3).

The real number of J parameters depends on the symmetry of the compound. For compounds **1**−**3**, which possess C_2 symmetry, four different J values should be taken into account (see below, Figure 5), but to avoid overparameterization we have considered the simplest two-J model, where $J_1 = J_2$ and $J_a = J_b = J_c = J_d$. It should be noted that, as a consequence of the crudeness of the model, the exchange interactions between the Ni(II) ions belonging to the $Ni(O)_2Ni$ square ring and between the Ni(II) ions pertaining to the (Ni−N−O−Ni−O−N) hexagonal rings are averaged in each case. To investigate the influence of the Ni(II) local anisotropy on the magnetic properties of Ni_4 cube complexes, we have performed simulations with the MAGPACK program[21] on the two-J model (absolute D values were varied between 0 and 4 cm^{-1}). The complexes have been considered to exhibit either strong AF between the Ni(II) ions, like **1** and **2**, or a dominant AF interaction like **3** based upon the shape of χ_M. In all cases, the results of the simulations clearly show that the influence of D is likely to be a very weak effect, and perhaps more pertinently one which is very difficult to evidence from magnetic susceptibility data. This is in accordance with results previously reported for chain[22] and dinuclear Ni(II) complexes[23] with strong AF interactions between the Ni^{2+} ions and D/J values less than 1. In view of the above considerations, the magnetic data were analyzed by using the following isotropic spin Heisenberg Hamiltonian, in which the local anisotropy of the Ni(II) ions was not taken into account:

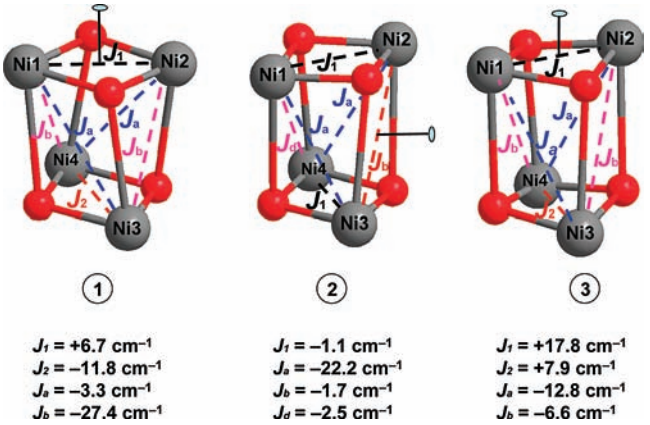

Figure 5. Simplified schemes of the J_i interactions and their corresponding DFT calculated values for compounds **1**−**3**.

$$H = -J_1(S_1S_2 + S_3S_4) - J_a(S_1S_3 + S_1S_4 + S_2S_3 + S_2S_4)$$

A parameter accounting for the percentage of paramagnetic impurity (ρ) was also considered. Very good fits were obtained by using the MAGPACK program[21] with the following parameters: $J_1 = -5.8$ cm^{-1}, $J_a = -22.1$ cm^{-1}, $g = 2.23$, and $\rho = 0.5\%$ for **1**; $J_1 = -2.4$ cm^{-1}, $J_a = -22.8$ cm^{-1}, $g = 2.24$, and $\rho = 1\%$ for **2**; $J_1 = +15.6$ cm^{-1}, $J_a = -10.8$ cm^{-1}, $g = 2.10$, and $\rho = 0.9\%$ for **3**. It should be highlighted that compound **3** represents the first example of an oximate-bridged homometallic Ni(II) complex where a ferromagnetic (hereafter F) interaction has been observed between Ni(II) ions mediated by double μ-*O* oximate bridges.

The values of J_a for **1**−**3**, which fall in the range −10.8 cm^{-1}/−22.8 cm^{-1}, are consistent with those reported for other oximate-bridged complexes containing μ_3-Ni−(O)(Ni)−N−Ni bridges.[5] The J_1 values deserve more detailed comment. In principle, the most important structural factors in determining

(21) (a) Borrás-Almenar, J. J.; Clemente, J.; Coronado, E.; Tsukerblat, B. S. *Inorg. Chem.* **1999**, *38*, 6081. (b) Borrás-Almenar, J. J.; Clemente, J.; Coronado, E.; Tsukerblat, B. S. *J. Comput. Chem.* **2001**, *22*, 985.

(22) Borrás-Almenar, J. J.; Coronado, E.; Curely, J.; Georges, R. *Inorg. Chem.* **1995**, *34*, 2699.

(23) Mandal, S.; Balamurugan, V.; Lloret, F.; Mukherjee, R. *Inorg. Chem.* **2009**, *48*, 7544.

Scheme 5. $[(NH_3)_4Ni(\mu\text{-}OH)_2Ni)(NH_3)]^{2+}$ Model Compound for the Calculations of J versus θ and τ Angles (Left), α Torsion Angle (Centre) and β Dihedral Angle (Right) Inside the Ni_4^{2+} Core

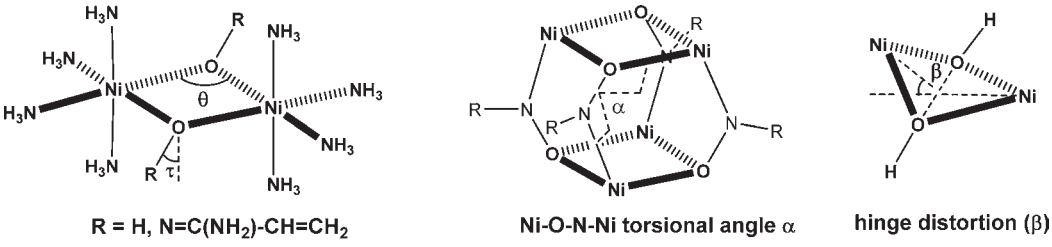

the nature of the magnetic exchange interactions in the $Ni(O)_2Ni$ unit should be the Ni−O−Ni bridging angle (θ) and the out-of-plane angle of the N atom of the NO oximate bridging group, with respect to the $Ni(O)_2Ni$ plane (τ angle, see Scheme 5). The M−O−M bridging angle has been shown to be the main factor affecting the nature of the magnetic exchange interaction in $M(O)_2M$ planar alkoxo[24] and phenoxo[25] copper(II) and nickel(II)[26] complexes (the AF coupling is favored when θ increases). Moreover, for planar $Cu(O)_2Cu$ complexes, it has been shown that the AF interaction increases when τ decreases.[27] In view of this, it is reasonable to assume that small θ angles (in the vicinity of 90−95°) combined with larger τ values (> 30−40°) should lead to weak AF or even F interactions. For complexes **1** and **2**, with θ and τ angles in the 99−100° and 62−67° ranges, respectively, weak AF interactions between the Ni(II) ions of the $Ni(O)_2Ni$ planar units would be expected, which is in good agreement with the observed values. For **3**, with θ angles (94.2° and 95.1°) that are significantly smaller than those observed for **1** and **2**, and large τ values of ∼57°, a very weak AF or F interaction would be expected, which again matches well with the observed F interaction. It is well-known that the *syn-syn* bridging coordination mode exhibited by benzoate groups in compound **3** causes AF coupling. However, if other bridges are also present, they could add (orbital complementarity) or counterbalance (orbital countercomplementarity) these effects.[28] In connection with this, it has been shown that *syn-syn* carboxylate bridges with either alkoxo,[23] hydroxo,[29] or water[30] bridging ligands, exhibit countercomplementarity leading to either F or very weak AF interactions. Therefore, the existence of the axial magnetic exchange pathway through the *syn-syn* benzoate bridge in **3** may also contribute (in addition to the smaller θ and larger τ angles) to the observed F interaction in this compound through orbital countercomplementarity. It should be noted that for the compound $[Ni_4(O_2CMe)_2\{(py)_2CNO\}_4](SCN)(OH)\cdot 2.2MeOH\cdot 1.7H_2O$,[5e] which has a similar structure to **3** with a *syn-syn* acetate group bridging the Ni(II) ions of each of the $Ni(O)_2Ni$ units of the Ni_4^{2+} core, and θ and τ values of ∼94° and ∼50°, respectively, J_1 was reported to be $-2.7\ cm^{-1}$. In this case, other structural factors, such as Ni−O distances, the folding of the $Ni(O)_2Ni$ unit, the Ni····Ni distances, the existence of *syn-syn* acetate bridges, and the distortion of the Ni(II) coordination sphere, and so forth, were not considered but may well lead to the observed very weak AF interaction. The experimental J values and some relevant structural parameters for complexes **1**−**3** and $[Ni_4(O_2CMe)_2\{(py)_2CNO\}_4](SCN)(OH)\cdot 2.2MeOH\cdot 1.7H_2O$ are summarized in Table 2.

To support the experimental values of J_1 and J_a for compounds **1**−**3**, to calculate the "remaining" possible J values for these compounds, and to demonstrate the feasibility of the ferromagnetic interaction in the $Ni(O)_2Ni$ units and its dependence on the θ and τ angles, DFT calculations were carried out on the X-ray structures as found in solid state as well as on model compounds.

The high spin (HS) and broken-symmetry states (BS) for each of the compounds as well the relationships derived from the difference between the energy of the HS state and that of the BS states, from which the J_i parameters can be calculated, are given in Supporting Information, Figures S1−S3. The scheme of interactions and the calculated J_i values for each compound are given in Figure 5. A close analysis of the DFT results allow some conclusions to be drawn: (i) the calculated J parameters, and more concretely their average values, agree in sign and rather well in magnitude with the experimental data; (ii) as expected, the sign and magnitude of the calculated J values seem to depend largely on some structural factors of the Ni_4^{2+} core: the θ and τ angles for the exchange interactions inside the $Ni(\mu\text{-}O)_2Ni$ square rings, and the Ni−N−O−Ni torsion angle, α (see Scheme 5) for the interactions propagated through the Ni−N−O(Ni)−Ni exchange pathways defining the side of the hexagonal rings.

In **1**, J_1 and J_2 (that represent the magnetic exchange interactions inside each of the $Ni(\mu\text{-}O)_2Ni$ units) are of opposite sign, the former being F ($+6.7\ cm^{-1}$) and the latter being AF ($-11.8\ cm^{-1}$). Since the τ values are virtually identical for the two $Ni(\mu\text{-}O)_2Ni$ units (average values of 63.5° and 63.2°), the difference in sign and magnitude may be mainly ascribed to the different values of θ in these units (99.6° and 100.7°). It appears from these magneto-structural data that for τ values near to 60°, the sign and magnitude of the magnetic interaction between Ni(II) ions connected by double $\mu\text{-}O_{oximate}$ bridges is very sensitive to small differences in the θ bridging angle. In **2**, the $Ni(\mu\text{-}O)_2Ni$ units are equal and asymmetric with θ angles of 100.6° and 99.1° and an average τ angle of 64.9°. In view of these values, the small AF magnetic interaction between Ni(II) ions inside the $Ni(\mu\text{-}O)_2Ni$ units ($J_1 = -1.1\ cm^{-1}$) is not unexpected. For **3**, as in **1**, the

(24) (a) Merz, L.; Haase, W. *J. Chem. Soc., Dalton Trans.* **1980**, 875. (b) Handa, M.; Koga, N.; Kida, S. *Bull. Chem. Soc. Jpn.* **1988**, *61*, 3853.
(25) Thompson, L. K.; Mandal, S. K.; Tandon, S. S.; Bridson, J. N.; Park, M. K. *Inorg. Chem.* **1996**, *35*, 3117.
(26) Nanda, K. K.; Thompson, L. K.; Bridson, J. N.; Nag, K. *J. Chem. Soc., Chem. Commun.* **1994**, 1337.
(27) (a) Ruiz, E.; Alemany, P.; Alvarez, S.; Cano, J. *J. Am. Chem. Soc.* **1997**, *119*, 1297. (b) Ruiz, E.; Alemany, P.; Alvarez, S.; Cano, J. *Inorg. Chem.* **1997**, *36*, 3683.
(28) (a) Nishida, Y.; Kida, S. *J. Chem. Soc., Dalton Trans.* **1986**, 2633. (b) McKee, V.; Zvagulis, M.; Reed, C. A. *Inorg. Chem.* **1985**, *24*, 2914.
(29) (a) Gutierrez, L.; Alzuet, G.; Real, J. A.; Cano, J.; Borrás, J.; Castiñeiras, A. *Inorg. Chem.* **2000**, *39*, 3608. (b) Gutierrez, L.; Alzuet, G.; Real, J. A.; Cano, J.; Borras, J.; Castiñeiras, A. *Eur. J. Inorg. Chem.* **2002**, *8*, 2094.
(30) Cañadillas-Delgado, L.; Fabelo, O.; Pasán, J.; Delgado, F. S.; Lloret, F.; Julve, M.; Ruiz-Pérez, C. *Inorg. Chem.* **2007**, *46*, 7458.

Table 2. Experimental J Values and Some Relevant Structural Parameters for Ni_4 Cube Shaped Complexes

complexes	J_{exp} (cm^{-1})[a] J_1	J_a	θ (deg)	τ (deg) range	α (deg) ranges	Ni···Ni (Å)[b]
1	−5.8	−22.1	100.7,99.6	62.7−64.1	38.2−39.7	3.179
					70.9−71.2	3.138
2	−2.4	−22.8	99.3, 100.2	62.8−66.7	34.1−41.6	3.168
			99.1, 100.6		68.3−73.0	3.165
3	+15.6	−10.8	94.2, 95.1	55.7−59.0	41.5−41.7	3.043
					68.3−69.2	3.015
$[Ni_4(O_2CMe)_2\{(py)_2CNO\}_4]$ $(SCN)(OH)\cdot 2.2MeOH\cdot 1.7H_2O$	−2.7	−12.1	94.0, 94.0	44.7−65.1	44.7−45.7	3.069
			93.5, 94.8		63.1−65.1	3.056

[a] Calculated using the *two-J* model. [b] Ni···Ni distances inside the $Ni(O)_2Ni$ units.

$\theta/\tau_{average}$ angles inside the two $Ni(\mu\text{-}O)_2Ni$ units are different, with values of 94.2°/57.5° and 95.1°/57.2°. Therefore, J_1 = +17.8 cm^{-1} would correspond to the former angles and J_2 = +7.9 cm^{-1} to the latter ones. To establish a quantitative magneto-structural correlation for bis(μ-$O_{oximate}$)dinickel(II) complexes, we have performed additional DFT calculations on the simple planar model $[(NH_3)_4Ni(\mu\text{-}OR)_2Ni)(NH_3)]^{2+}$ as shown in Scheme 5.

We have calculated the J values on two planar models (R = H and R = N=C(NH_2)CH=CH_2, namely, OH and oxim models, respectively) by varying the θ angle in the range 80°−105° for two different τ values (30° and 60°). The aim of these calculations is to know how the magnetic exchange coupling between the Ni(II) ions inside the $Ni(\mu\text{-}O)_2Ni$ square rings depends not only on θ and τ but also on the type of bridge (either hydroxo or oximate). The results are represented in Figure 6.

As can be observed, first, the J values for the bis(oximate)-dinickel(II) model are in general bigger than those for the bis(hydroxo)dinickel(II) one. Moreover, the difference in J values increases with increasing τ. Second, for τ = 30° and regardless of the θ angle and type of bridge, all magnetic interactions are AF, and the magnitude of the AF interaction increases when θ increases for angles bigger than 90°. On the other hand, when the τ angle increases the AF interaction diminishes and becomes ferromagnetic. The change from AF to F occurs with θ values smaller than 96.5° and 100° for the OH and oximate models, respectively, and τ angles in the 30−60° range. The larger ferromagnetic interaction is predicted for θ close to 90° and τ close to 60°. It is worthy of remark that for θ values larger than 90° and τ values below 60°, the curves show a large slope. This may be the reason why the experimental J values in this region are very sensitive to small changes in θ and τ values.

We have also calculated J_1 for the compound $[Ni_4(O_2CMe)_2\{(py)_2CNO\}_4](SCN)(OH)\cdot 2.2MeOH\cdot 1.7H_2O$,[5e] which exhibited an unexpected AF interaction inside the $Ni(\mu\text{-}O)_2Ni$ square rings (see above). The calculated value J_1 = −5.6 cm^{-1} agrees well with the sign of the experimental value (J_1 = −2.7 cm^{-1}), thus showing the reliability of the DFT calculations for this kind of tetranuclear Ni(II) compound. To gauge the influence of the folding angle β (the dihedral angle between the O−Ni−O planes of the $Ni(\mu\text{-}O)_2Ni$ square ring) on the magnetic exchange interaction inside the $Ni(\mu\text{-}O)_2Ni$ unit, we have performed calculations of how J_1 varies with the β angle using the model complex $[(NH_3)_4Ni(\mu\text{-}OR)_2Ni)(NH_3)]^{2+}$ (R= H) shown in Scheme 5. We have considered for two θ values (95° and 100°) and three β values (0,° 10°, and 20°). The results are gathered in Table 3.

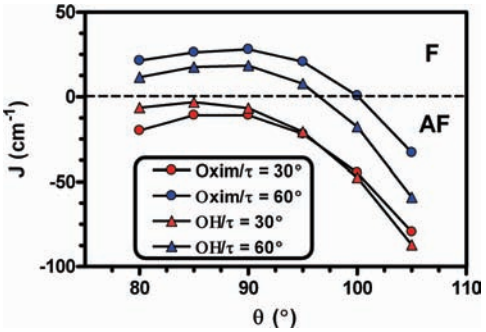

Figure 6. Dependence of the J values with θ and τ angles for the model compound $[(NH_3)_4Ni(\mu OR)_2Ni)(NH_3)]^{2+}$ (R = H for OH and R = N=C(NH_2)CH=CH_2 for oxim)

Table 3. Calculated J_1 Values versus β Angles for Two Different Values of θ

β/(deg)	J_1/cm^{-1} (θ = 95°)[a]	J_2/cm^{-1} (θ = 100°)[a]
0	+7.8	−17.7
10	−14.4	−42.4
20	−23.5	−53.9

[a] For τ = 60°

As expected, these results clearly show that, on the one hand, the magnitude of the AF interaction increases as β increases, and on other, the increase in the AF interaction is larger when θ increases. The folding angle observed for the compound $[Ni_4(O_2CMe)_2\{(py)_2CNO\}_4]$-$(SCN)(OH)\cdot 2.2MeOH\cdot 1.7H_2O$,[5e] ($\beta$ = 29.1°) may well explain why it exhibits an AF interaction instead of the expected ferromagnetic interaction for θ and τ values of ~94° and ~50°.

When the *syn-syn* benzoate groups in **3** are substituted by four non-bridging water molecules, J_1 and J_2 decrease from +17.8 cm^{-1} and +7.9 cm^{-1} to +11.8 cm^{-1} and +5.7 cm^{-1}, respectively. This result is good supporting evidence for the contercomplementarity effect caused by the *syn-syn* bridging benzoate ligand. Nevertheless, the magnitude of this effect seems to be less important than the dependence of J_1 and J_2 on θ, τ, and β angles, since J_1 and J_2 clearly remain ferromagnetic after the removal of the benzoate groups (see Table 3 and Figure 6).

As for the J parameters describing the magnetic exchange interactions through the α Ni−N−O(Ni)−Ni exchange pathways that define the sides of the hexagonal rings of the Ni_4^{2+} core, there is a clear (and expected) correlation associated with a σ interaction between the nickel(II) magnetic orbitals via the N−O bond (see Scheme 6): the

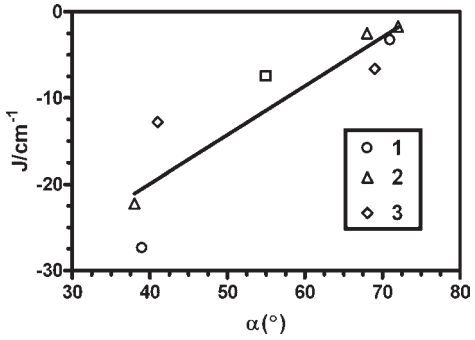

Figure 7. Calculated magnetic exchange couplings for **1**−**3** and $[Ni_4(O_2CMe)_4\{(py)C(Ph)NO\}_4]$ (SCN)(OH)·2.2MeOH·1.7H_2O.[5e] The solid line represents the theoretical linear relationship between the calculated J and α values.

Scheme 6. Representation of the Nickel(II) $d_{x^2-y^2}$ and d_{z^2} Magnetic Orbitals and p Oximate Orbitals Involved in the σ Ni−N−O(Ni)−Ni Exchange Pathway

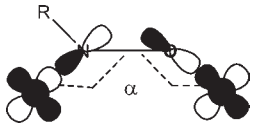

larger the Ni−N−O−Ni torsion angle, α, the lower the AF interaction.

Thus, for **1**, $J_b = -27.4$ cm^{-1} corresponds to the magnetic exchange pathways defining the more regular hexagonal rings with α∼39°, whereas $J_a = -3.3$ cm^{-1} is ascribed to the magnetic interaction mediated by the exchange pathways that define the sides of the less regular hexagonal rings with α ∼71°. In **2**, $J_a = -22.2$ cm^{-1} is ascribed to the exchange pathways with α ∼35° and ∼41°, whereas $J_b = -1.7$ cm^{-1} and $J_d = -2.5$ cm^{-1} correspond to α ∼72° and α ∼68°, respectively. Finally, for **3**, $J_a = -12.8$ cm^{-1} and $J_b = -6.6$ cm^{-1} involve the exchange pathways with α ∼41° and α ∼69°, respectively. From these values and the calculated $J_a = -7.5$ cm^{-1} for the $[Ni_4(O_2CMe)_4\{(py)C(Ph)NO\}_4](SCN)(OH)\cdot 2.2MeOH\cdot 1.7H_2O$[5e] (the four hexagonal rings have almost the same couple of α angles, with an average value of 55°), an almost linear relationship between J and α can be obtained (Figure 7). The crossover point from AF to F interactions is predicted at α ∼ 75°, whereas the maximum value of the AF interaction is expected for α = 0 with $J \sim -43$ cm^{-1}.

Concluding Remarks

The use of two carboxamideoxamidate ligands, bipyridine-2-carboxamideoxime (HL) and pyrimidine-2-carboxamideoxime, (HL1) has allowed us to prepare three examples of an unusual oximate-bridged Ni_4 complex. In these clusters, L^- and $L1^-$ ligands exhibit κ^3-N1,N8,N15:κ^1-O16:κ^1-O16 and κ^2-N1,N9:κ-O10:κ-O10 chelating/bridging modes, respectively, generating two almost square-planar $Ni(O)_2Ni$ rings and four irregular hexagonal $Ni(NO)_2Ni$ rings inside the Ni_4^{2+} unit, that can be considered as a cube with single [O-atom] and double [NO oxime] bridging groups as atom edges. The magnetic results for compounds **1**−**3** clearly show that the magnetic exchange interactions inside the Ni(μ-$O)_2$Ni square rings may be AF or F depending on the Ni−O−Ni bridging angle (θ) and the out-of-plane angle of the NO oximate bridging group with respect to the $Ni(O)_2Ni$ plane (τ), whereas the interactions propagated through the Ni−N−O(Ni)−Ni exchange pathways defining the side of the hexagonal rings are AF and depend on the Ni−N−O−Ni torsion angle (α). In **3**, the *syn-syn* bridging coordination of the benzoate ligand to the Ni(II) ions of the same $Ni(O)_2Ni$ square planar ring gives rise to a considerable decrease in the θ angles (94.2° and 95.1°), which are significantly smaller than those observed for **1** and **2** (τ is rather large ∼57°), and F interactions are observed. The existence of the axial magnetic exchange pathway through the *syn-syn* benzoate bridge may also contribute (in addition to the θ and τ angles) to the observed F interaction in compound **3** through the orbital countercomplementarity effect.

DFT calculations have allowed the establishment of a magneto-structural correlation between J and the angles θ and τ for the planar model compounds $[(NH_3)_4Ni(\mu OR)_2Ni)(NH_3)]^{2+}$ (R = H and R = N=C(NH_2)CH=CH_2, namely, OH and oxim models, respectively) by varying the θ angle in the range 80°−105° for two different τ values (30° and 60°). The correlation shows the following: (i) the J values for the bis(oximate)dinickel(II) model are in general larger than those for the bis(hydroxo)dinickel(II) model. Moreover, the difference in the J values increases with increasing τ. (ii) For τ = 30° and regardless of the θ angle and type of bridge, all magnetic interactions are AF, and the magnitude of the AF interaction increases when θ increases for angles bigger than 90°. (iii) When the τ angle increases the AF interaction diminishes and becomes ferromagnetic. The change from AF to F occurs with θ values smaller than 96.5° and 100° for the OH and oxim models, respectively, and τ angles in the 30−60° range. The larger ferromagnetic interaction is predicted for θ close to 90° and τ close to 60°, and (iv) For θ values larger than 90° and τ values below 60°, the curves show a large slope. This may be the reason why the experimental J values in this region are very sensitive to small changes in θ and τ values.

To know the magnitude of the countercomplementarity effect promoted by the *syn-syn* benzoate group in **3**, we have performed DFT calculations on a molecule derived from **3** by substitution of the two *syn-syn* benzoate groups by four non-bridging water molecules. This substitution causes J_1 and J_2 to decrease from +17.8 cm^{-1} and +7.9 cm^{-1} to +11.8 cm^{-1} and +5.7 cm^{-1}, respectively. This result suggests that the magnitude of countercomplementarity effect is less important than the dependence of J_1 and J_2 on θ, τ, and β angles (see Table 3).

For the J parameters describing the magnetic exchange interactions through the α Ni−N−O(Ni)−Ni exchange pathways that define the sides of the hexagonal rings of the Ni_4^{2+} core, an almost linear correlation between J and α can be established. From this correlation, the crossover point from AF to F interactions is predicted at α ∼ 75°, whereas the maximum value of the AF interaction is expected for α = 0 with $J \sim -43$ cm^{-1}.

To support our theoretical results, and particularly those for the magnetic exchange interactions inside the Ni(μ-$O)_2$Ni square rings, more examples of Ni_4 clusters analogous to **3** are needed. We are now pursuing the synthesis of these systems by changing benzoate for other carboxylates and other bidentate bridging ligands, and pyrazine by other ancillary *N*-donating ligands. We thus expect to access a large number of compounds with smaller θ and large τ angles that exhibit F interactions inside the Ni(μ-$O)_2$Ni square rings. We are also using both carboxamideoxime ligands and azide in reactions

with nickel(II) ions with the aim of obtaining high nuclearity clusters possessing high spin ground states. Finally, the change of the solvent and the use hydrothermal and/or microwave methods may provide a number of other HL and HL1-containing high-nuclearity Ni(II) complexes with subtle differences in their core. Work is in progress along these lines.

Acknowledgment. This work was supported by the MEC (Spain) (Project CTQ-2008-02269/BQU), the Junta de Andalucía (FQM-195 and Projects of excellence P08-FQM-03705 and P07-FQM-03092) and the University of Granada. M.A.P thanks the Ministerio de Ciencia e Innovación of Spain for a FPI grant. Financial support from the University of Granada and Junta de Andalucia for the visit of E.C. to the University of Edinburgh is grateful acknowledged. We would like to thank the Centro de Supercomputación de la Universidad de Granada for computational resources and Dr. Joan Cano, University of Valencia, Spain, for his continuous and generous assistance with the DFT calculations. E.K.B. would like to thank the EPSRC and Leverhulme Trust for financial support.

Supporting Information Available: Crystallographic data in CIF format, and Figures S1-S3. This material is available free of charge via the Internet at http://pubs.acs.org.

Note Added after ASAP Publication. This paper was published on the Web on October 1, 2010, with an error in equation 3. The corrected version was reposted on October 5, 2010.